The Study of Designing Electro-Photo Catalytic Reactor with Photovoltaic Cells for Wastewater Treatment

Ali Ataya Yasser Alhchaimi[1], Shaymaa Hamzah Algabri[2]

[1]Al-Muthanna University, College of Engineering, Department of Chemical Engineering, alialzarqany80@gmail.com
[2]Al-Qadisiyah University, College of Engineering, Department of Mechanical Engineering, Shaymaa.hamza@qu.edu.iq

This paper assesses the efficiency of various electrode combinations in treating Refinery Wastewater (RWW) using electrocatalytic oxidation (ECO) to determine the optimal operating conditions in the reactor, specifically focusing on energy consumption for organic removal. The Box-Behnken experimental design and ANOVA analysis were employed for this investigation. The applied potential across all electrodes was identified as the most influential operating parameter. X-ray diffraction analysis confirmed the typical crystalline nature of the by-products formed, which were predominantly amorphous or poorly crystalline in structure. During the Electrochemical Sequential Chlorination (ESC) process, various oxidants including active chlorine species and oxidizing radicals were generated, contributing to the oxidation of organic compounds in the aqueous solution. Additionally, the functional groups present in zinc oxide were characterized using Fourier Transform Infrared (FT-IR) spectroscopy. The study yielded a maximum organic removal efficiency of 98.2%. Furthermore, it was observed that the operating conditions of the electrodes exhibited similar trends in specific energy consumption (SEC) for organic removal, with an energy consumption of 39.11 kWh/m^3.

Keywords: Solar Energy; photovoltaic; Wastewater Treatment; Advanced Oxidation Processes; Electro-catalytic.

1. Introduction

Solar energy is a clean and abundant resource that can be harnessed for various applications such as providing warmth, light, and power aimed at both national and manufacturing use [1]. However, with the rapid depletion of conservative resources of energy like petroleum, fuel, and natural gas, along with the ecological squalor caused by their extraction and use, there's an urgent need to shift towards renewable energy sources [2]. Solar energy presents a promising solution to meet future energy demands sustainably while mitigating greenhouse gas emissions. Despite the immense potential of solar energy, its efficient utilization remains a challenge due to the limited efficiency of solar cell arrays. Solar energy can be converted

into electricity or heat using two main technologies: photovoltaic systems and solar collectors [3],[4]. These technologies are widely employed for commercial and residential applications, offering clean and renewable alternatives to conventional energy sources. In the context of global economic development, new energy technologies, including solar energy, are becoming increasingly pivotal [5],[6]. Governments worldwide are recognizing the importance of solar energy as a key component of their sustainable development strategies. Photovoltaic power generation stands out for its safety, reliability, lack of noise and pollution, low failure rate, and ease of maintenance. In developing countries, the adoption of solar photovoltaic (PV) panels has surged, driven by fluctuations in oil prices [7]. Solar PV generators offer diverse applications and significant benefits, particularly in remote areas where decentralized energy supply is crucial [8] . These systems provide affordable and secure electrical sources, independent of centralized power plants[9],[10]. However, industrial development has led to increased oil usage, resulting in the generation of oil-polluted wastewater from various sources such as crude oil production, refineries, petrochemical industries, and others [11],[12] . Treating refinery wastewater typically involves membrane [13] , biosynthesis [14], adsorption [15],[16] and oxidation procedures [17], with advanced oxidation processes (AOPs) emerging as effective techniques [18],[19] . AOPs utilize solar light as a cost-effective alternative to UV/O_3 and granular-activated carbon processes, facilitating the complete mineralization of organic pollutants into CO_2, H_2O, and inorganic components [20],[21]. Electro-catalytic oxidation (ECO) for wastewater treatment involves using electrodes coated with catalysts to facilitate the oxidation of organic pollutants [22]. This study focuses on oil elimination from RWW through ECO, optimizing agent dose, and studying the effects of current, pH, and electrolysis time on the ECO process.

2. Materials and methods

2.1 Substances and Organic Test

The wastewater is polluted with organic pollutants analyst. The RWW remained stowed in a container of polypropylene at a lower temperature to remain treated by ECO treatment. Table 1 shows the RWW properties. All substances rummage-sale in this paper remained of analytical grade and were not cleansed additional. H_2SO_4 (SDFCL 98% purity), Zinc Oxide (99% India), NaOH, and CCl_4 and sodium chloride from India are all examples of these compounds. In a separating funnel, 0.2 grams of NaCl were added to 40 ml of reclaimed wastewater (RWW) to disrupt any organic emulsion present in the sample. Subsequently, 4 ml of CCl_4 was added to the mixture in the separating funnel. The mixture was vigorously shaken aimed at 2 minutes to ensure thorough mixing. After shaking, the solution was allowed to stand for 30 minutes to facilitate phase separation. Two distinct layers, an upper aqueous layer, and a lower organic layer, formed in the separating funnel. The inferior (organic) layer, containing the extracted substance, was carefully separated from the aqueous layer. The organic layer was then analyzed using a UV-1800 spectrophotometer to determine the presence and concentration of the desired substance.

Table 1 Specification of RWW

Parameters	Values	Parameters	Values
Oil content	105.2 (mg/l)	**Conductivity**	100521 µs/cm)
Turbidity	45.1 NTU	**TDS**	64333.44 (mg/l)
pH	6.75	**Viscosity**	1.0215/S
Solution oxygen Content	0.042 (mg/l)	**Iron**	0.33 (mg/l)
Specific gravity	0.997	**Sulphate**	55.2 (mg/l)

2.2. Photovoltaic cell: The photovoltaic cell consists of four acrylic blocks assembled together with sheets of silicon rubber gaskets placed between them to prevent leaks. This configuration allows for two possible anode locations within the anolyte section: either at the end-plate (between the acrylic blocks where the anode will be z1 cm distant from the cathode, as illustrated in Fig. 1)

Fig. 1 – : Main parts of the flow-cell.

2.3. Electro oxidation reactor:

The experimental reactor comprised a power supply, stainless steel anode, iron cathode, aerator, and an electrocatalytic cell, as depicted in Figure 2. The electrocatalytic oxidation cell was constructed from quartz glass measuring 250 x 280 x 160 mm. The anode, a self-made stainless steel electrode plate, was integrated into the cell, while the cathode was a commercially sourced iron plate. These electrodes were connected to the power supply to set up the reactor. The reactor adopted an improved parallel structure with a shared-anode and double electrolytic cells, consisting of one anode plate and two cathode plates. The effective area of the anode plate immersed in the solution measured 250 x 250 x 2 mm. This design effectively doubled the treatment capacity for organic pollutants in RWW without increasing the electrolytic cell area, thereby enhancing the utilization efficiency of the anode plate. The reactor was operated by applying power for 10 minutes to sweep iron ions, followed by the addition of ZnO doses with agitation speed as depicted in Figure 2. Samples were collected at regular intervals, centrifuged at 2000 rpm for 15 minutes to separate the sludge, and the supernatant was collected for organic estimation. Produced water reduction was calculated as the ratio of residual oil at time t (Ct) to initial oil (C0). Further experiments were conducted by varying the current, ZnO dosage, and time. Prior to use in the ECO process, the electrodes were thoroughly cleaned with water to remove any debris. Subsequently, they were soaked in 1N HCl for 1 hour followed by 1M NaOH for another hour.

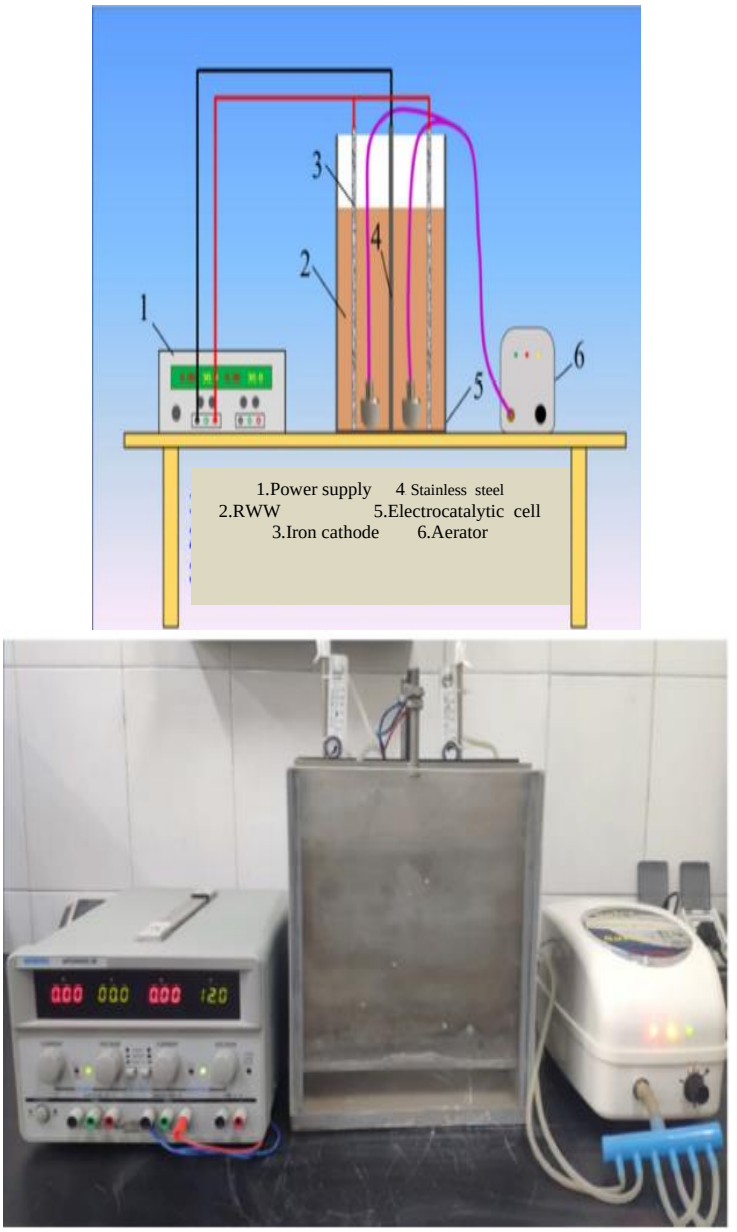

Figure 2. Experimental device.

In addition, the energy consumption (measured in kWh/m3) emerges as a critical aspect in these treatment methodologies. Therefore, it was computed using the following equation :

$$E = (U.I.t)/(1000V) \quad (1)$$

Here, U represents the applied voltage (in volts), I denotes the applied current (in Amperes), t stands for the contact time (in hours), and V signifies the volume of the refinery wastewater

(in cubic meters)

2.4. Experimental design : In this study, the optimization of experimental conditions for direct red wastewater mineralization and decolonization via the ECO process was achieved using the Box-Behnken design method within the framework of Response Surface Methodology (RSM). The software Design Expert Minitab-17 was utilized for the experimental design, data analysis, extraction of the quadratic model, and plotting of graphs. The independent variables considered were current (X_1), ZnO dose (X_2), electrolysis time (X_3), and pH (X_4). These variables were coded at low and high levels according to the Box-Behnken design, as presented in Table 2

Table 2: Operational parameters

Parameters	Ranges
X_1: current (Amps)	0..5-1.5
X_2: ZnO dose (gm)	0.25-1
X_3: electrolysis time (min)	5-30
X_4: pH	3-9

3. Results and discussion

3.1 Characterization of zinc oxide

X-Ray diffraction (XRD) was used to investigate the crystalline phase and structural integrity of the samples. The peaks shape and location may supply knowledge about the structure of crystalline, material grain size , material phase nature and lattice parameter, among other things. In Figure 3 the XRD of ZnO peaks indexed at 2Θ= 25.270 , 36.910, 37.771, 38.528, 48.010, 53.849, 55.037, 62.073, 62.649.the robust deflection peaks at 25.27 and 48.01 denoting ZnO in the anatase phase. The intensity of XRD peaks of the example reflects that the shaped particles are crystal-like and comprehensive deflection peaks specify very minor size crystallite [23].

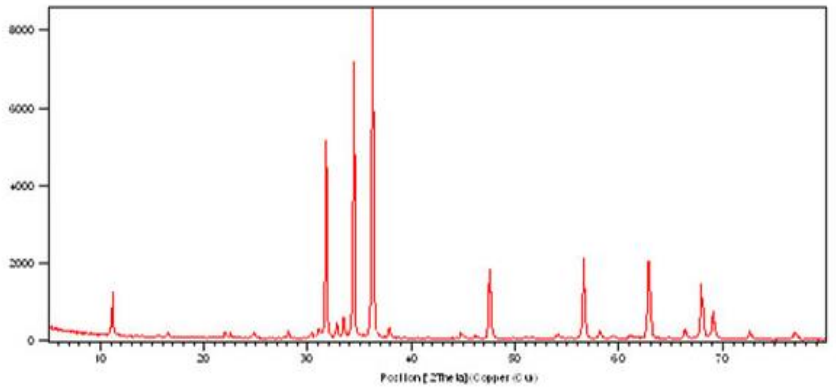

Figure 3: XRD pattern of ZnO nanoparticles

Fourier transform infrared spectroscopy test remained showed by means of a Shimadzu FTIR spectrometer model No: 8400S under ambient conditions, spanning the range from 4000 to 400 cm−1. The FTIR spectra of the ZnO nanomaterial are presented in Figure 4. Particle size distribution was determined using photon correlation spectroscopy. Morphological features and dimensional changes were observed under a scanning electron microscope [24],[25].

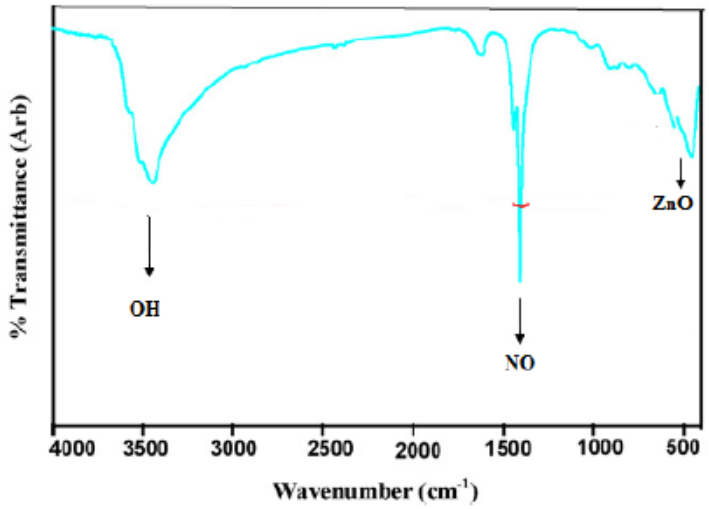

Fig. 4. FTIR spectra of ZnO nanomaterial

3.2 Statistical examination

A statistically designed industrial test comprising twenty-seven experiments was conducted to improve and evaluate the combined effects of independent variables on a wide range of process parameters. The quality of these process limits was assessed using Minitab-17 software. The independent variables for wastewater treatment are outlined in Table 3.

Table 3. BBD for organic examination

Run	StdOrder	RunOrder	PtType	Blocks	Current (Amps)	ZnO dose (gm)	Electrolysis time (min)	pH	Y_{OCRE}
1	1	1	2	1	0.5	0.25	17.5	6	75.4
2	2	2	2	1	1.5	0.25	17.5	6	87.4
3	3	3	2	1	0.5	1	17.5	6	90.2
4	4	4	2	1	1.5	1	17.5	6	91.8
5	5	5	2	1	1	0.625	5	3	95.3
6	6	6	2	1	1	0.625	30	3	98.4
7	7	7	2	1	1	0.625	5	9	84.1
8	8	8	2	1	1	0.625	30	9	88.6
9	9	9	2	1	0.5	0.625	17.5	3	79.1
10	10	10	2	1	1.5	0.625	17.5	3	89.8
11	11	11	2	1	0.5	0.625	17.5	9	68.7
12	12	12	2	1	1.5	0.625	17.5	9	73.1
13	13	13	2	1	1	0.25	5	6	65.9

14	14	14	2	1	1	1	5	6	78.5
15	15	15	2	1	1	0.25	30	6	73.5
16	16	16	2	1	1	1	30	6	85.1
17	17	17	2	1	0.5	0.625	5	6	71.8
18	18	18	2	1	1.5	0.625	5	6	78.6
19	19	19	2	1	0.5	0.625	30	6	76.2
20	20	20	2	1	1.5	0.625	30	6	81.4
21	21	21	2	1	1	0.25	17.5	3	82.5
22	22	22	2	1	1	1	17.5	3	87.1
23	23	23	2	1	1	0.25	17.5	9	74.3
24	24	24	2	1	1	1	17.5	9	85.6
25	25	25	0	1	1	0.625	17.5	6	80.4
26	26	26	0	1	1	0.625	17.5	6	81
27	27	27	0	1	1	0.625	17.5	6	80.9

The consequence of trials to inspect an untried association between organic removal subsequent quadratic classical remained used to achieve development variables and express in terms of actual units [8] :

$$\text{Organic Removal} = 69.8 + 36.6\,X_1 + 18.9\,X_2 + 0.23\,X_3 - 6.55\,X_4 - 6.9\,X_1^2 + 0.1\,X_2^2 + 0.0002\,X_3^2 + 0.408\,X_4^2 - 13.9\,X_1X_2 - 0.064X_1X_3 - 1.05\,X_1X_4 - 0.053\,X_2X_3 + 1.49\,X_2X_4 + 0.009\,X_3X_4 \quad (2)$$

Equation (2) was formulated to quantify the efficiency of organic removal in refinery wastewater. The positive constants in the equation indicate that removal increases with the corresponding effects of these coefficients. Specifically, changes in amps, dosage, and time positively influence organic removal. The efficacy of this equation was rigorously determined through ANOVA testing. Table 4, which outlines organic removal in RWW, was constructed based on the results of the F-test and P-test. These statistical tests provide insights into the significance of the coefficients and their impact on organic removal efficiency.

Table 4 ANOVA for Organic removal

Foundation	DOF	Seq. SS	Adj. MS	Fisher Value	P–test Value
1-Model	14	955.31	68.237	1.17	0.4
Linear	4	779.57	194.892	3.33	0.047
X_1	1	138.04	138.041	2.36	0.151
X_2	1	293.04	293.041	5	0.045
X_3	1	70.08	70.083	1.2	0.295
X_4	1	278.4	278.403	4.75	0.05
Square	4	126.18	31.545	0.54	0.71
X_1^2	1	15.64	15.641	0.27	0.615
X_2^2	1	0	0.001	0	0.997
X_3^2	1	0	0.003	0	0.994
X_4^2	1	72.03	72.03	1.23	0.289
2-Way Interaction	6	49.57	8.261	0.14	0.988
X_1*X_2	1	27.04	27.04	0.46	0.51
X_1*X_3	1	0.64	0.64	0.01	0.918
X_1*X_4	1	9.92	9.923	0.17	0.688
X_2*X_3	1	0.25	0.25	0	0.949
X_2*X_4	1	11.22	11.223	0.19	0.669
X_3*X_4	1	0.49	0.49	0.01	0.929

Error	12	702.85	58.571		
Lack-of-Fit	10	702.65	70.265	679.98	0.001
Pure ErroR	2	0.21	0.103		
Total	26	1658.17			

3.1.1 The current effect:

The electric potential difference and the intensity of the current applied to the electrode are crucial parameters in electrocatalytic wastewater treatment processes. To examine the effect of current on the presentation of the electrocatalytic process, experiments were conducted at currents of 0.5, 1, and 1.5 mA. It was experiential that organic elimination augmented with cumulative current, reaching an all-out of 86.2% at a current of 1.5 mA (Fig. 5). Lower removal efficiencies were achieved at currents ≤0.5 mA, with removal rates of 89.1% at 0.6 mA, 87.2% at 0.4 mA, and 76.1% at 0.5 mA, as depicted in Fig. 4. A higher current lead to a higher production rate of oxidation on the cathode surface. Consequently, more free hydroxyl radicals accumulate in the bulk solution, resulting in greater organic degradation [26]. However, increasing the current beyond 1 mA did not significantly enhance oil removal during the 20–30-minute period. Similar trends have been observed in the electrocatalytic treatment of organic [27].

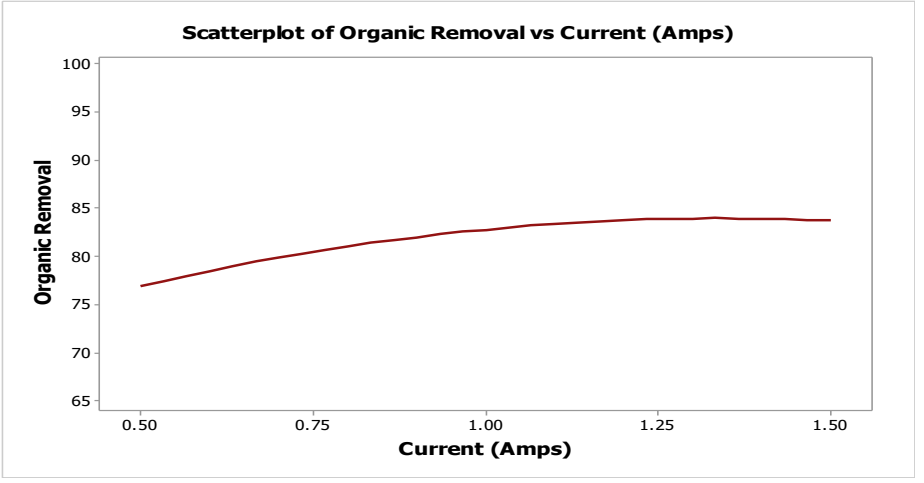

Fig. 5. The current effect on the organic elimination

3.1.2 Zinc oxide effect

The dosage level is a critical factor in the degradation of organic pollutants, such as the organic content in refinery wastewater (RWW). It plays a significant role in the generation of hydroxyl radicals (●OH), which are crucial for catalytic oxidation processes [28]. Figure 6 illustrates the effects of dosage ranging from 0.25 to 1 gram on refinery wastewater. The effectiveness of ZnO as an electrocatalyst relies on various factors, including its surface structure, morphology, and the specific reaction under consideration [29]. ZnO nanoparticles or nanostructures typically possess high surface areas, which can significantly enhance their electrocatalytic activity by providing numerous active sites for oxidation reactions to occur [30]. These active sites facilitate the adsorption and activation of reactant molecules, promoting efficient catalytic oxidation processes [31].

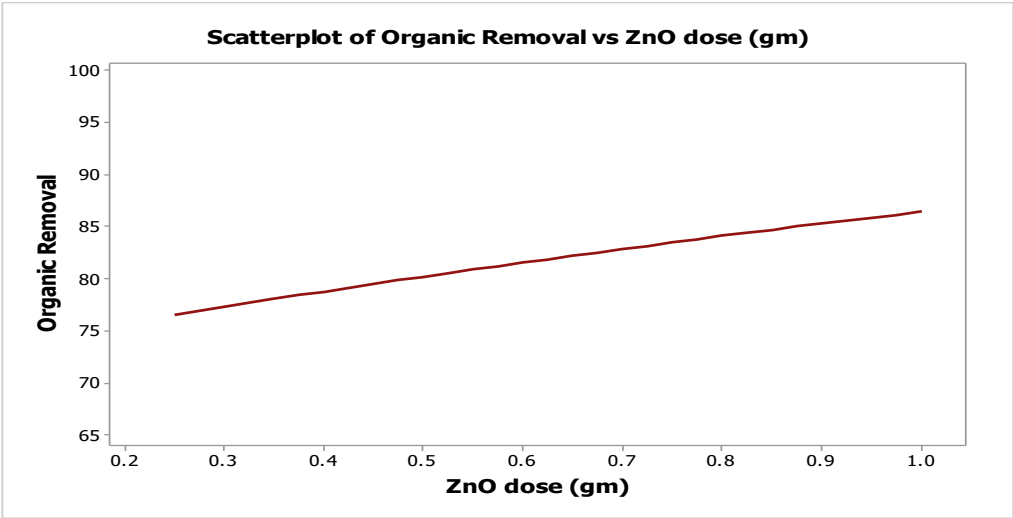

Fig. 6. The dose effect on oil elimination.

3.1.3 Electrolysis time effect:

To assess the impact of electrolysis time, experiments were conducted under consistent operating conditions corresponding to a 105.2 ppm oil content in refinery wastewater (RWW). As depicted in Fig. 7, the percentage of organic removal exhibited a steep increase with the reaction time up to ten minutes, reaching a maximum of 84.1%. However, beyond this point, there was no significant improvement in organic removal percentage. The observed trend in organic removal percentage can be attributed to changes in pollutant concentration in the wastewater undergoing electrochemical treatment. This finding is consistent with the study by the lecture [32]. The longer the electrolysis time, the higher the efficiency of organic pollutants removal from the RWW, primarily due to the increased activity of the adsorption process occurring throughout the electrochemical reactor as the electrolysis time is extended [33].

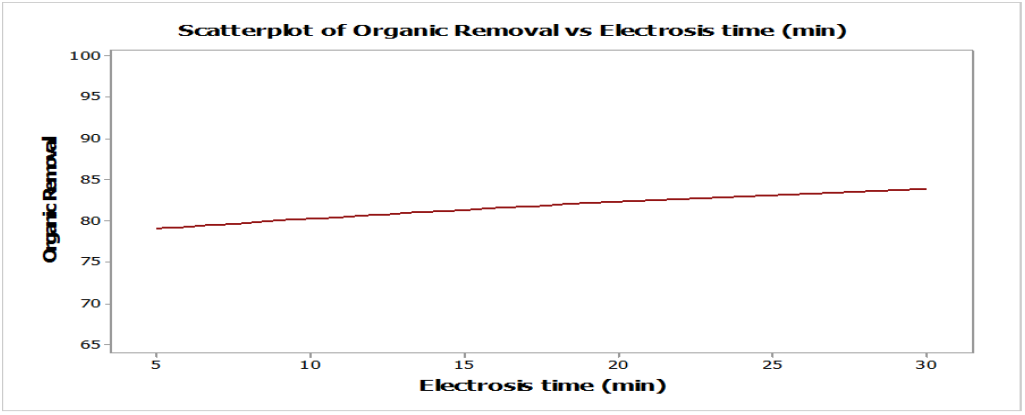

Fig. 7. The electrolysis time effect on oil elimination

3.1.4 Effect of pH:

The effect of initial pH was investigated at a constant current, with pH values ranging from 3 to 9 and a treatment time of 30 minutes for both stainless steel (SS) and iron (Fe) electrodes. The influence of initial pH on organic removal percentages for both types of electrodes is depicted in Fig. 8 [34]. The findings indicate that organic removal efficiency was higher at acidic pH levels, which aligns with the results obtained in this study. Previous research has also demonstrated temporal patterns of total organic carbon removal percentage in relation to pH values, showing a significant decrease in treatment efficiency with increasing pH values. Thus, it can be concluded that the electrochemical process is more effective under acidic conditions compared to alkaline conditions. These results suggest that the production rate of radicals for reducing organic pollutants in wastewater is higher in acidic solutions compared to alkaline solutions [35]. However, it is important to note that any increase in acidity should be carefully managed in consideration of the coating applied on the anode and cathode to prevent corrosion of these coatings [36].

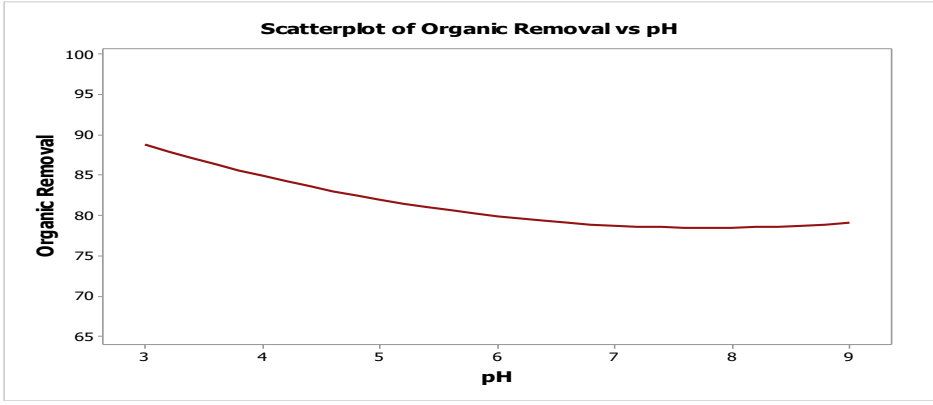

Fig. 8. The pH effect on oil elimination

3.3 Best of working variables

The optimal values for current, electrolysis time, and pH remained determined by means of a statistical software program . Figure 9 illustrates the outcomes of the D-optimization analysis. The optimized values resulted in organic compound removal efficiencies exceeding 98%.

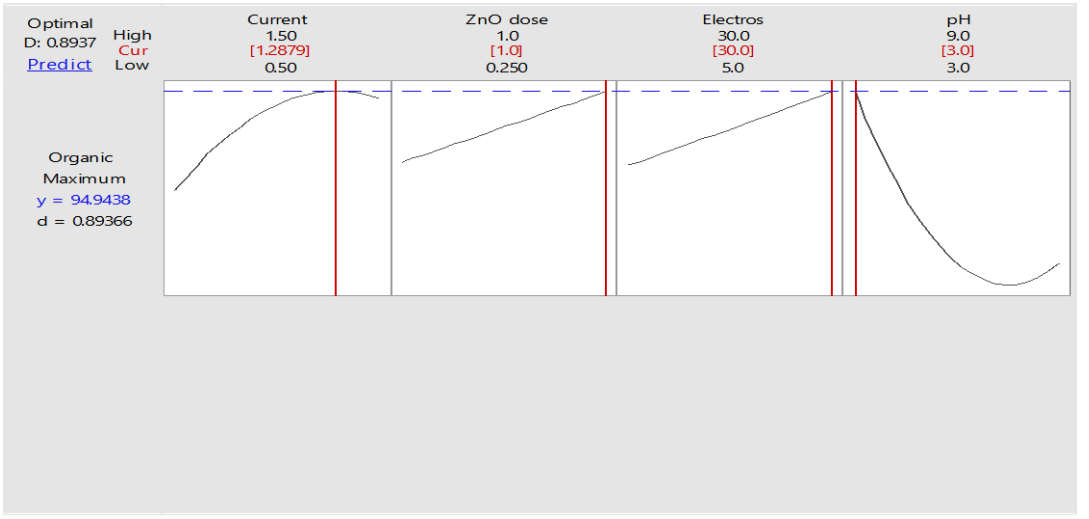

Fig. 9. The Best values of the working variables.

3.4 Estimation of energy consumption

Efforts to minimize power costs should focus on reducing energy expenditure, which includes both electrolysis and the drive of solution or electrodes. The project of electrodes and the cell plays a crucial role in achieving this goal. Utilizing open flow-through porous electrodes can minimize pressure drops, resulting in lower driving prices and easier reactor closing. Additionally, electrodes with high surface areas can promote turbulence in bed electrodes, leading to temperately high mass transfer coefficients and lively areas deprived of requiring high flow rates through the cell, thus further reducing pumping costs [37]. The adoption of electrocatalytic knowledge for effluent treatment necessitates consideration of several factors, including the performance of anode substance, the consumption of power, and working costs. Figure 10 illustrates the relationship between energy consumption, electrolysis time, and current during the electrocatalytic action of organic content in RWW. It is observed that energy consumption values are relative to the applied current and time across all types of water during ECO treatment [38] .

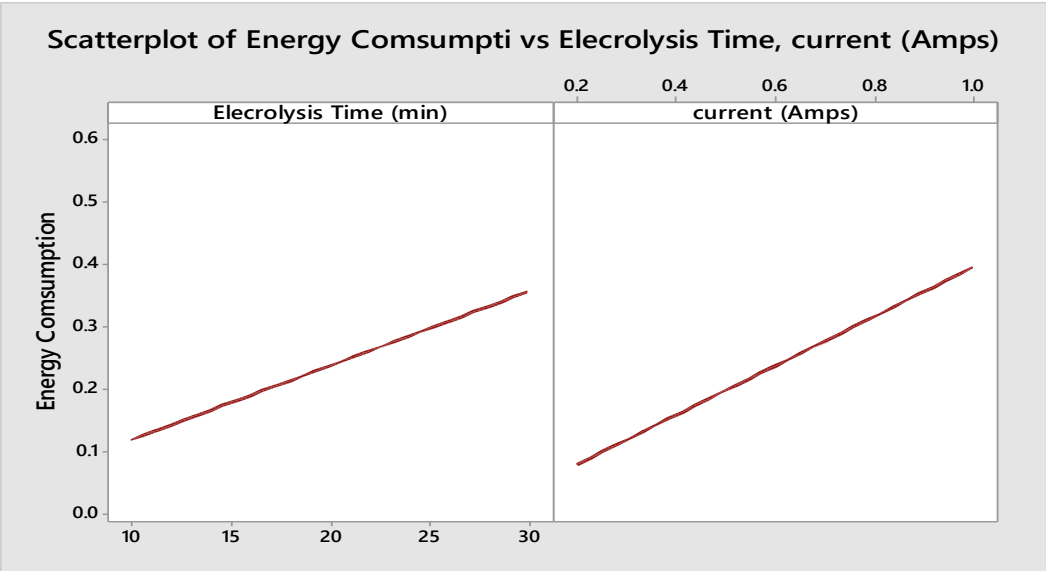

Fig. 10. The result of the working variables on the power consumption

Based on the optimal values of current and time previously strongminded, the energy and electrode consumption were calculated . Figure 10 illustrates the consumption of energy by way of a function of the active variables throughout the ECO process for contaminant removal. Observations indicate that energy consumption increases more sharply with current compared toward the upsurge with time. This suggests that current plays a more important role in determining energy consumption, a finding supported by existing literature [39].

4. Conclusion

The electrocatalytic treatment of fluid containing organic pollutants has been investigated under various operating conditions, including current, zinc dose, initial pH, and treatment time. Optimization of operational conditions for oil removal, current efficiency, hydrogen peroxide generation, and electrolysis time was attained using RSM based on BBD, aiming to achieve high oil removal efficiency while minimizing energy consumption. The all-out organic elimination competence of 98.2% was attained under the following optimized conditions: electrolysis time of 30 minutes, at 3 pH, current of 1.5 Amps, and 1 gram of zinc oxide dosage. Nano-porosity plays a crucial role in facilitating the degradation of ZnO, ultimately promoting the formation of free radicals. Given the exceptional performance of ECO operation, this technique holds promise for treating refinery wastewater effectively.

References

[1] T. B. Pavón-Silva, H. Romero-Tehuitzil, G. M. Del Río, and J. Huacuz-Villamar, “Photovoltaic energy-assisted electrocoagulation of a synthetic textile effluent,” Int. J. Photoenergy, vol. 2018, 2018, doi: 10.1155/2018/7978901.

[2] Y. Al-Douri and F. M. Abed, “Solar energy status in Iraq: Abundant or not - Steps forward,” J. Renew. Sustain. Energy, vol. 8, no. 2, 2016, doi: 10.1063/1.4947076.

[3] J. M. Vindel, E. Trincado, and A. Sánchez-Bayón, “European union green deal and the opportunity cost of wastewater treatment projects,” Energies, vol. 14, no. 7, pp. 1–18, 2021, doi: 10.3390/en14071994.

[4] K. A. Alakoul, A. S. Atiyah, M. Z. Azeez, and A. A. Hassan, " Photovoltaic cell Electro-Oxidation for Oil Removal in oil field produced H 2 O ," IOP Conf. Ser. Mater. Sci. Eng., vol. 1090, no. 1, p. 012072, 2021, doi: 10.1088/1757-899x/1090/1/012072.

[5] S. Alsadi, "applied sciences Status : A Review of Criteria , Constrains , Models , Techniques , and Software Tools." 2018.

[6] H. R. D. Alamery, A. A. Hassan, and A. H. Rashid, "Copper Removal in Simulated Wastewater by Solar Fenton Oxidation," AIP Conf. Proc., vol. 2806, no. 1, 2023, doi: 10.1063/5.0167259.

[7] C. O. Assembe, "Integrated solar photovoltaic and thermal system for enhanced energy efficiency." pp. 36–75, 2016.

[8] S. F. Alturki, A. H. Ghareeb, R. T. Hadi, and A. A. Hassan, "Evaluation of Using Photovoltaic Cell in the Electro-Fenton Oxidation for the Removal of Oil Content in Refinery Wastewater," IOP Conf. Ser. Mater. Sci. Eng., vol. 1090, no. 1, p. 012012, 2021, doi: 10.1088/1757-899x/1090/1/012012.

[9] R. D. Nsaif, S. F. Alturki, M. S. Suwaed, and A. A. Hassan, "Lead removal from refinery wastewater by using photovoltaic electro Fenton oxidation," in AIP Conference Proceedings, AIP Publishing, 2023.

[10] M. K. Ibrahim, A. A. Al-Hassan, and A. S. Naje, "Utilisation of cassia surattensis seeds as natural adsorbent for oil content removal in oilfield produced water," Pertanika J. Sci. Technol., vol. 27, no. 4, pp. 2123–2138, 2019.

[11] G. F. Naser, I. H. Dakhil, and A. A. Hasan, "Organic pollutants removal from oilfield produced water using nano magnetite as adsorbent," Glob. NEST J., vol. 23, no. 3, pp. 381–387, 2021, doi: 10.30955/gnj.003875.

[12] A. H. Rashid, A. A.hassan, R. T. Hadi, and A. S. Naje, "Treatment of oil content in oilfield produced water using chemically modified waste sawdust as biosorbent," Ecol. Environ. Conserv., vol. 26, no. 4, pp. 1563–1571, 2020.

[13] O. Iglesias, M. J. Rivero, A. M. Urtiaga, and I. Ortiz, "Membrane-based photocatalytic systems for process intensification," Chem. Eng. J., vol. 305, pp. 136–148, 2016, doi: 10.1016/j.cej.2016.01.047.

[14] S. Jaroenpoj, J. Yu, and J. Ness, "Development of artificial neural network models for biogas production from co-digestion of leachate and pineapple peel," Glob Env. eng, vol. 1, pp. 42–47, 2015.

[15] A. A. Hassan, R. T. Hadi, A. H. Rashid, and A. S. Naje, "Chemical modification of castor oil as adsorbent material for oil content removal from oilfield produced water," Pollut. Res., vol. 39, no. 4, pp. 892–900, 2020.

[16] A. Saleh Jafer and A. A. Hassan, "Removal of oil content in oilfield produced water using chemically modified kiwi peels as efficient low-cost adsorbent," J. Phys. Conf. Ser., vol. 1294, no. 7, 2019, doi: 10.1088/1742-6596/1294/7/072013.

[17] A. A. Hassan, H. T. Naeem, and R. T. Hadi, "A Comparative Study of Chemical Material Additives on Polyacrylamide to Treatment of Waste Water in Refineries," IOP Conf. Ser. Mater. Sci. Eng., vol. 518, no. 6, p. 62003, 2019, doi: 10.1088/1757-899X/518/6/062003.

[18] K. M. Mousa Al-Zobai and A. A. Hassan, "Utilization of Iron Oxide Nanoparticles (Hematite) as Adsorbent for Removal of Organic Pollutants in Refinery Wastewater," in Materials Science Forum, Trans Tech Publ, 2022, pp. 91–100.

[19] H. T. Naeem, A. A. Hassan, and R. T. Al-Khateeb, "Wastewater-(Direct red dye) treatment-using solar fenton process," J. Pharm. Sci. Res., vol. 10, no. 9, pp. 2309–2313, 2018.

[20] A. S. Jafer, R. Al-Khateeb, B. Alobaid, A. Atiyah, and A. A. Hassan, "Copper removal from produced water by photo Fenton oxidation," in AIP Conference Proceedings, AIP Publishing, 2023.

[21] A. A. Hassan, F. Y. AlJaberi, and R. T. AL-Khateeb, "Batch and Continuous Photo-Fenton

Oxidation of Reactive-Red Dye from Wastewater," J. Ecol. Eng., vol. 23, no. 1, pp. 14–23, 2022.

[22] I. H. Ahmed, A. A. Hassan, and H. K. Sultan, "Study of Electro-Fenton Oxidation for the Removal of oil content in refinery wastewater," IOP Conf. Ser. Mater. Sci. Eng., vol. 1090, no. 1, p. 012005, 2021, doi: 10.1088/1757-899x/1090/1/012005.

[23] P. Yekan Motlagh, B. Vahid, S. Akay, B. Kayan, Y. Yoon, and A. Khataee, "Ultrasonic-assisted photocatalytic degradation of various organic contaminants using ZnO supported on a natural polymer of sporopollenin," Ultrason. Sonochem., vol. 98, no. April, p. 106486, 2023, doi: 10.1016/j.ultsonch.2023.106486.

[24] S. B. Farise, H. A. Alabdly, and A. A. Hasan, "Lead Removal from Simulated Wastewater Using Magnetite As Adsorbent with Box-Behnken Design," IOP Conf. Ser. Earth Environ. Sci., vol. 790, no. 1, 2021, doi: 10.1088/1755-1315/790/1/012020.

[25] H. T. Naeem and A. A. Hassan, "Effectiveness & economy of sawdust wood adsorbents in removing anionic dyes of aqueous solutions," Pakistan J. Biotechnol., vol. 15, no. 2, pp. 311–320, 2018.

[26] F. I. El-Hosiny, K. A. Selim, M. A. A. Khalek, and I. Osama, "Produced Water Treatment Using a New Designed Electroflotation Cell," Int. J. Res. Ind. Eng. , vol. 6, no. 4, pp. 328–338, 2017, doi: 10.22105/riej.2017.100959.1022.

[27] H. A. Ibrahim, A. A. Hassan, A. H. Ali, and H. M. Kareem, "Organic removal from refinery wastewater by using electro catalytic oxidation," in AIP Conference Proceedings, AIP Publishing, 2023.

[28] H. R. D. Alamery and A. A. Hassan, "Effect of intensity of light and distance for decolonization in direct red wastewater by photo fenton oxidation," ARPN J. Eng. Appl. Sci., vol. 17, no. 1819–6608, p. 9, 2006.

[29] A. A. Hassan and K. M. M. Al-Zobai, "Chemical oxidation for oil separation from oilfield produced water under uv irradiation using titanium dioxide as a nano-photocatalyst by batch and continuous techniques," Int. J. Chem. Eng., vol. 2019, 2019, doi: 10.1155/2019/9810728.

[30] H. K. Sultan, H. Y. Aziz, B. H. Maula, A. A. Hasan, and W. A. Hatem, "Evaluation of Contaminated Water Treatment on the Durability of Steel Piles," vol. 2020, p. 1269563, 2020.

[31] K. M. M. Al-zobai, A. A. Hassan, and N. O. Kariem, "Removal of amoxicillin from polluted water using UV/TiO2, UV/ZnO/TiO2, and UV/ZnO," Solid State Technol., vol. 63, no. 3, pp. 3567–3575, 2020.

[32] F. Y. AlJaberi, B. A. Abdulmajeed, A. A. Hassan, and M. L. Ghadban, "Assessment of an Electrocoagulation Reactor for the Removal of Oil Content and Turbidity from Real Oily Wastewater Using Response Surface Method," Recent Innov. Chem. Eng. (Formerly Recent Patents Chem. Eng., vol. 13, no. 1, pp. 55–71, 2020, doi: 10.2174/2405520412666190830091842.

[33] T. R. Devlin, M. S. Kowalski, E. Pagaduan, X. Zhang, V. Wei, and J. A. Oleszkiewicz, "Electrocoagulation of wastewater using aluminum, iron, and magnesium electrodes," J. Hazard. Mater., pp. 862–868, 2019, doi: 10.1016/j.jhazmat.2018.10.017.

[34] A. Baiju, R. Gandhimathi, S. T. Ramesh, and P. V. Nidheesh, "Combined heterogeneous Electro-Fenton and biological process for the treatment of stabilized landfill leachate," J. Environ. Manage., vol. 210, pp. 328–337, 2018, doi: 10.1016/j.jenvman.2018.01.019.

[35] S. Saeid et al., "Pt modified heterogeneous catalysts combined with ozonation for the removal of diclofenac from aqueous solutions and the fate of by-products," Catalysts, vol. 10, no. 3, 2020, doi: 10.3390/catal10030322.

[36] W. Z. Khan, I. Najeeb, M. Tuiyebayeva, and Z. Makhtayeva, "Refinery wastewater degradation with titanium dioxide, zinc oxide, and hydrogen peroxide in a photocatalytic reactor," Process Saf. Environ. Prot., vol. 94, no. C, pp. 479–486, 2015, doi:

10.1016/j.psep.2014.10.007.

[37] A. S. Atiyah, A. A. A. Al-Samawi, and A. A. Hassan, "Photovoltaic cell electro-Fenton oxidation for treatment oily wastewater," AIP Conf. Proc., vol. 2235, no. May, 2020, doi: 10.1063/5.0008937.

[38] H. Afanga et al., "Integrated electrochemical processes for textile industry wastewater treatment: System performances and sludge settling characteristics," Sustain. Environ. Res., vol. 30, no. 1, pp. 1–11, 2020, doi: 10.1186/s42834-019-0043-2.

[39] Y. J. Chen et al., "Application of fenton method for the removal of organic matter in sewage sludge at room temperature," Sustain., vol. 12, no. 4, pp. 1–10, 2020, doi: 10.3390/su12041518.